Propionic-Acid-Terminated Silicon Nanoparticles: Synthesis and Optical Characterization

Seiichi Sato[†,‡] and Mark T. Swihart*[,†]

Department of Chemical and Biological Engineering, University at Buffalo (SUNY), Buffalo, New York 14260-4200, and Graduate School of Material Science, University of Hyogo, 3-2-1 Koto, Kamigori-cho, Ako-gun, Hyogo 678-1297, Japan

Received March 30, 2006

Photoinitiated hydrosilylation was used to attach acrylic acid to the surface of photoluminescent silicon nanoparticles, thereby producing water-dispersible, propionic-acid-terminated particles. From transmission electron microscope (TEM) observations, the average diameters of the synthesized nanocrystals were 1.9−2.4 nm. It is likely that smaller particles (<1.5 nm) were also present but could not be imaged. As the nanocrystal size decreased, both the optical absorption edge and photoluminescence (PL) emission peak blue-shifted, whereas the photoluminescence excitation (PLE) spectrum changed very little and showed a sharp onset indicative of direct interband absorption at Γ. After prolonged ultrasonication in water, the Si nanoparticles showed strong blue PL. This can tentatively be attributed to the formation of radiative centers related to incomplete oxidation of the nanocrystals. The silicon nanocrystals could be transferred into water or methanol by dialysis without inducing this oxidation. The PA-terminated Si nanoparticles were stably dispersed in acrylic acid, water, and methanol and showed essentially the same optical properties in all three solvents. The approach used here provides a general means of producing water-dispersible silicon nanocrystals with size-dependent photoluminescence tunable over a wide range of the visible spectrum.

Introduction

Making nanoparticles dispersible in water is an important step toward making them more useful in the fields of biological, optical, and electronic engineering. According to Derjaguin−Landau−Verwey−Overbeek (DLVO) theory,[1,2] interaction between nanoparticles in aqueous suspensions can be widely varied from repulsion to attraction by changing the pH. This allows systematic control of the dispersion and assembly of nanoparticles in aqueous suspensions. Stably dispersed nanoparticles have promise as fluorescence probes in bioimaging.[3,4] Nanoparticle superlattices,[5−13] which can be made by slowly assembling nanoparticles from a suspension, are interesting electronic materials for potential applications ranging from ultrahigh density memories to emitters for solid-state lighting and displays. Although self-assembly from organic solvents can be controlled by adjusting the solvent composition, the simple pH-based tunability of interaction that is possible in aqueous dispersions cannot readily be achieved in other solvents.

Water-dispersible nanoparticles of various materials such as CdSe[3,4] and Au[13,14] have been synthesized by modifying the particle surfaces to provide hydrophilic termination with amine, carboxyl, or other groups. However, those nanoparticles are not necessarily suitable for all applications. For example, although CdSe nanoparticles show bright visible luminescence, they contain Cd, which has high potential toxicity. Au nanoparticles are innocuous and stable, but they cannot be used for light-emitting materials and the source material may be too costly for some potential applications. Silicon nanoparticles have the potential to overcome these limitations.[15−24] Si is inert, nontoxic, abundant, and economi-

* Corresponding author. Phone: (716) 645-2911, ext. 2205. Fax: (716) 645-3822. E-mail: swihart@eng.buffalo.edu.
† University at Buffalo (SUNY).
‡ University of Hyogo.

(1) Israelachvili, J. N. *Intermolecular and Surface Forces*; Academic Press: London, 1992.
(2) Hunter, R. J. *Foundations of Colloid Science*, 2nd ed.; Oxford University Press: Oxford, U.K., 2001.
(3) Bruchez, M., Jr.; Moronne, M.; Gin, P.; Weiss, S.; Alivisatos, A. P. *Science* **1998**, *281*, 2013−2015.
(4) Chan, W. C. W.; Nie, S. *Science* **1998**, *281*, 2016−2018.
(5) Murray, C. B.; Kagan, C. R.; Bawendi, M. G. *Annu. Rev. Mater. Sci.* **2000**, *30*, 545−610.
(6) Collier, C. P.; Vossmeyer, T.; Heath, J. R. *Annu. Rev. Phys. Chem.* **1998**, *49*, 371−404.
(7) Taleb, A.; Petit, C.; Pileni, M. P. *Chem. Mater.* **1997**, *9*, 950−959.
(8) Harfenist, S. A.; Wang, Z. L.; Alvarez, M. M.; Vezmar, I.; Whetten, R. L. *J. Phys. Chem.* **1996**, *100*, 13904−13910.
(9) Shevchenko, E.; Talapin, D.; Kornowski, A.; Wiekhorst, F.; Kotzler, J.; Haase, M.; Rogach, A.; Weller, H. *Adv. Mater.* **2002**, *14*, 287.
(10) Shevchenko, E. V.; Talapin, D. V.; Rogach, A. L.; Kornowski, A.; Haase, M.; Weller, H. *J. Am. Chem. Soc.* **2002**, *124*, 11480−11485.
(11) Stoeva, S. I.; Prasad, B. L. V.; Uma, S.; Stoimenov, P. K.; Zaikovski, V.; Sorensen, C. M.; Klabunde, K. J. *J. Phys. Chem. B* **2003**, *107*, 7441−7448.
(12) Sato, S.; Yao, H.; Kimura, K. *Physica E* **2003**, *17*, 521−522.
(13) Sato, S.; Wang, S.; Kinugasa, S.; Yao, H.; Kimura, K. In *Physics, Chemistry and Application of Nanostructures*; Borisenko, V. E., Gaponenko, S. V., Gurin, V. S., Eds.; World Scientific: Hackensack, NJ, 2003; p 313.
(14) Chen, S. H.; Kimura, K. *Langmuir* **1999**, *15*, 1075−1082.
(15) Takagi, H.; Ogawa, H.; Yamazaki, Y.; Ishizaki, A.; Nakagiri, T. *Appl. Phys. Lett.* 1990, 56, 2379−2380.
(16) Wilcoxon, J. P.; Samara, G. A.; Provencio, P. N. *Phys. Rev. B* **1999**, *60*, 2704−2714.
(17) Ledoux, G.; Gong, J.; Huisken, F.; Guillois, O.; Reynaud, C. *Appl. Phys. Lett.* **2002**, *80*, 4834−4836.
(18) Li, X.; He, Y.; Talukdar, S. S.; Swihart, M. T. *Langmuir* **2003**, *19*, 8490−8496.
(19) Liu, S.-m.; Sato, S.; Kimura, K. *Langmuir* **2005**, *21*, 6324−6329.

10.1021/cm060750t CCC: $33.50 © 2006 American Chemical Society
Published on Web 07/22/2006

cal. Silicon nanocrystals can show visible luminescence at wavelengths spanning the visible spectrum[18,20,22,25−27]. However, preparation of water-dispersible silicon nanoparticles that maintain their size-dependent photoluminescence has proven difficult. Thus, there remains a need for an effective and practical means of making the silicon nanoparticle surfaces hydrophilic, similar to the surface modification of Au nanocrystals with strongly hydrophilic molecules, such as carboxylic acids,[14] that can allow the formation of stable aqueous dispersions. Water-dispersible silicon nanocrystals have recently been reported by Li and Ruckenstein[28,29] and by Warner et al.[30] However, each of those reports shows water-dispersible particles of a single emission color, and there are reasons to expect that neither can be applied to particles with emission across the visible spectrum. Li and Ruckenstein attached acrylic acid to the surface of silicon nanoparticles and demonstrated their potential as biological staining agents with tremendous photostability. However, they presented results only for red-emitting silicon nanoparticles whose FTIR spectrum showed substantial surface oxidation.[29] Such particles probably cannot be produced with yellow or green photoluminescence, because of the presence of oxygen-related states within the band gap.[20,31] In contrast, Warner et al. attached allylamine to silicon nanoparticles to provide an amino-terminated surface.[30] They also demonstrated the potential of these particles as photostable bioimaging agents. However, they presented results only for blue-emitting nanoparticles. Reaction with allylamine is not expected to be generally applicable to particles with longer emission wavelengths because of the quenching of silicon photoluminescence by amine groups.[32,33]

The aim of this study is to synthesize water-dispersible Si nanoparticles that show strong luminescence of various colors by terminating the nanocrystal surfaces with propionic acid (PA). The sizes, surface modification, and optical properties of the synthesized Si nanoparticles were evaluated by TEM imaging, FTIR spectroscopy, UV−Vis absorption, and PL and PLE measurements.

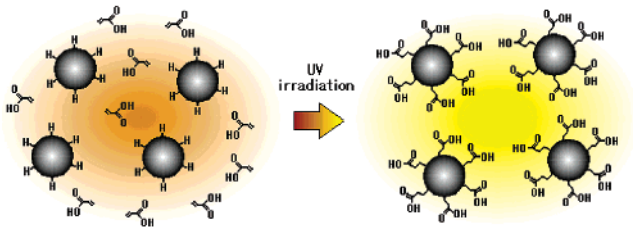

Figure 1. Schematic representation of the hydrosilylation of Si nanoparticles in acrylic acid. Surface Si atoms of the nanoparticles change from H to PA termination under UV illumination.

Experimental Section

Isolated Si nanocrystals were prepared as follows. Si-rich suboxide (SiO_x, $x = 0.6$) powder supplied by DENKA (Tokyo, Japan) was used as the starting material. This SiO_x powder contains a large number of Si nanocrystals 10 nm or more in diameter. First, 30 mg of the SiO_x powder was dispersed in 4 mL of methanol. A mixture of HF (49 wt %) and HNO_3 (69 wt %) (10/1 v/v) was then added, and the mixture was sonicated for 0.5−18 min using a Branson 2510R-DTH sonicator (100W, 40 kHz). This process rapidly dissolved the oxide and dispersed the Si nanocrystals that had been confined in the SiO_x powder and then more slowly decreased the Si nanocrystal sizes. As shown below, the silicon nanocrystal size decreased with increasing total etching time. The etched Si particles are hydrophobic, because the surface Si atoms are mostly terminated with hydrogen (H) atoms. Therefore, the Si particles remain loosely assembled in the suspension after sonication. These assemblies were collected on a polyvinylidene fluoride (PVDF) membrane filter (pore size 0.1 μm) and washed three times with methanol.

The H termination of the Si nanocrystals was transformed to PA termination (Figure 1) by photoinitiated hydrosilylation.[20,34] The hydrosilylation process proceeded as follows. The Si nanoparticles on the PVDF filter were immersed in a mixture of acrylic acid (99.5 wt %, stabilized) and HF (49 wt %) (4/1 v/v) and sonicated to thoroughly redisperse the particles. Mixing HF into acrylic acid was found to be essential in making the hydrosilylation process reproducible. This is presumably due to the rapid removal, by HF etching, of any surface oxide formed on the particles during hydrosilylation. We also tried to remove oxygen from the nanoparticle-containing acrylic acid by repeated freeze−thaw cycles under vacuum[20] instead of using HF. However, this was not sufficient to make the hydrosilylation reproducible. Whereas freeze−thaw cycles are expected to be quite effective in the removal of oxygen and other dissolved gases, this process cannot be expected to remove water contamination. Experimentally, HF addition was simpler than, and preferable to, elaborate solvent drying and degassing. Oxidation observed in the absence of HF may also have been due to reaction of the hydrogen-terminated silicon nanocrystals with the carboxyl group of the acrylic acid. To initiate hydrosilylation, we exposed the sample to ultraviolet (UV) light (254 nm) for 2−12 h using a Rayonet photochemical reactor (Southern New England Ultraviolet Co.) equipped with 6 RPR-2537 Å UV tubes. The suspension was continuously stirred during UV exposure. As shown below, the appearance of the nanoparticle suspensions changed from turbid to clear after the UV exposure. Some precipitates appeared after completion of the hydrosilylation process and were removed using a poly(tetrafluoroethylene) (PTFE) syringe filter (pore size 0.45 μm).

(20) Hua, F.; Swihart, M. T.; Ruckenstein, E. *Langmuir* **2005**, *21*, 6054−6062.
(21) Yang, C.-S.; Bley, R. A.; Kauzlarich, S. M.; Lee, H. W. H.; Delgado, G. R. *J. Am. Chem. Soc.* **1999**, *121*, 5191−5195.
(22) English, D. S.; Pell, L. E.; Yu, Z. H.; Barbara, P. F.; Korgel, B. A. *Nano Lett.* **2002**, *2*, 681−685.
(23) Belomoin, G.; Therrien, J.; Smith, A.; Rao, S.; Twesten, R.; Chaieb, S.; Nayfeh, M. H.; Wagner, L.; Mitas, L. *Appl. Phys. Lett.* **2002**, *80*, 841−843.
(24) Yamani, Z.; Ashhab, S.; Nayfeh, A.; Thompson, W. H.; Nayfeh, M. *J. Appl. Phys.* **1998**, *83*, 3929−3931.
(25) Holmes, J. D.; Ziegler, K. J.; Doty, R. C.; Pell, L. E.; Johnston, K. P.; Korgel, B. A. *J. Am. Chem. Soc.* **2001**, *123*, 3743−3748.
(26) Wilson, W. L.; Szajowski, P. J.; Brus, L. *Science* **1993**, *262*, 1242−1244.
(27) Littau, K. A.; Szajowski, P. J.; Muller, A. J.; Kortan, A. R.; Brus, L. *J. Phys. Chem.* **1993**, *97*, 1224−1230.
(28) Li, Z. F.; Ruckenstein, E. *Nano Lett.* **2004**, *4*, 1463−1467.
(29) Ruckenstein, E.; Li, Z. F. *Adv. Colloid Interface Sci.* **2005**, *113*, 43−63.
(30) Warner, J. H.; Hoshino, A.; Yamamoto, K.; Tilley, R. D. *Angew. Chem., Int. Ed.* **2005**, *44*, 4550−4554.
(31) Wolkin, M. V.; Jorne, J.; Fauchet, P. M.; Allan, G.; Delarue, C. *Phys. Rev. Lett.* **1999**, *82*, 197−200.
(32) Kirkey, W. D.; Sahoo, Y.; Li, X.; He, Y.; Swihart, M. T.; Cartwright, A. N.; Bruckenstein, S.; Prasad, P. N. *J. Mater. Chem.* **2005**, *15*, 2028−2034.
(33) Lauerhaas, J. M.; Credo, G. M.; Heinrich, J. L.; Sailor, M. J. *J. Am. Chem. Soc.* **1992**, *114*, 1911−1912.
(34) Buriak, J. M. *Chem. Rev.* **2002**, *102*, 1271−1308.

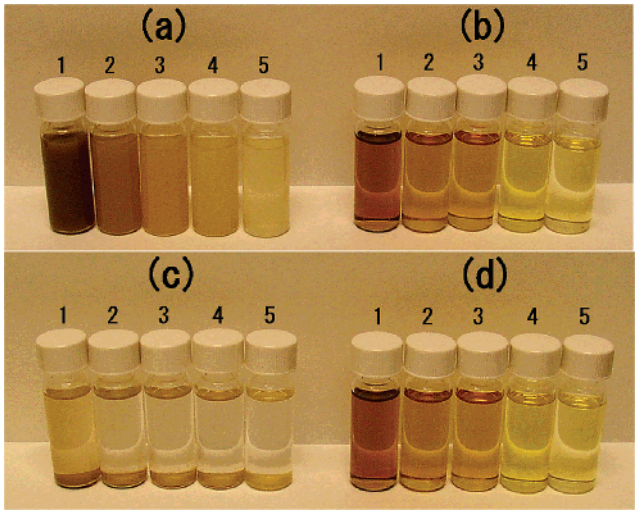

Figure 2. Comparison of silicon nanoparticle in acrylic acid (a) without UV exposure and (b) after UV exposure. Parts (c) and (d) show the same samples after 1 week of storage. The surface-modified particles are unchanged, whereas the particles not exposed to UV illumination have precipitated. The five samples labeled 1−5 were prepared by etching the starting $SiO_{0.6}$ for 0.5, 8, 10, 15, and 18 min, respectively.

The PA-terminated Si nanocrystals were observed with a JEM-2010 transmission electron microscope (TEM) operated at 200 kV. The current density of the electron beam was 20 ± 5 pA/cm^2 during the observations. The specimens were prepared for TEM observation by depositing droplets of the nanocrystal-containing suspensions onto amorphous carbon-coated TEM grids that were then dried at room temperature in air. Surface termination of the nanocrystals was evaluated with a Mattson Galaxy series 5000 Fourier transform infrared (FTIR) spectrometer. Optical absorption measurements were carried out with a Thermo Spectronic Genesys 6 UV−vis spectrophotometer. Photoluminescence (PL) and PL excitation (PLE) spectra were collected using a Perkin−Elmer LS50 luminescence spectrometer. The excitation wavelength for PL measurements was 360 nm.

Results and Discussion

The Si nanoparticles before and after UV exposure are shown in panels a and b of Figure 2, respectively. Samples 1−5 were produced by increasing the etching time from 30 s to 18 min. A color change, which is attributed to both an increase in band-gap energy and a decrease in particle volume fraction, is observed with increasing etching time. As seen in the difference between panels a and b of Figure 2, the samples change from turbid to clear in appearance after the UV exposure. After 1 week elapsed, samples a and b became c and d, respectively. As shown in Figure 2c, the nanoparticles that were not exposed to UV light were precipitated, but those exposed to UV light remained a clear, colloidally stable dispersion (Figure 2d).

Figure 3 shows TEM images of the Si nanocrystals after hydrosilylation. The samples in Figure 3a−c correspond to the samples 1−3, respectively, in Figure 2b. We were unable to image nanocrystals less than 1.5 nm in diameter, because the contrast between those nanocrystals and the background, an amorphous carbon film, was insufficient to allow accurate definition of the boundaries of the nanocrystals. We were unable to image any clearly identifiable nanocrystals in samples 4 and 5. Thus, it appears that nearly all of the nanoparticles in both sample 4 and 5 were less than 1.5 nm in diameter as a result of the long etching times used in their preparation. The average diameters obtained from the TEM images of Figure 3a−c are 2.4, 2.1, and 1.9 nm, respectively. However, these average diameters for images b and c are probably overestimates, because the size distributions suggest that a large number of Si particles less than 1.5 nm are present but not cannot be imaged and counted. As shown in the insets of images a and b, the lattice spacing observed in the nanocrystals was 3.1 Å, which corresponds to the (111) lattice spacing in bulk Si.

The FTIR spectra of the Si nanoparticles are shown in Figure 4. The gray-colored regions in the figure indicate wave number ranges in which peaks attributed to carboxyl groups and C−H bonds appear.[14,35] The green, red, and blue regions are the ranges in which peaks attributed to C═C, Si−CH_2, and Si−O bonds appear, respectively.[21,35] For comparison, an experimental spectrum from pure acrylic acid is shown as curve a. Except for spectrum a, all measurements were made on dried samples. An FTIR spectrum of the Si nanoparticles after hydrosilylation is shown in spectrum b. A comparison of spectra a and b shows that peaks attributed to C═C bonds are clearly present in spectrum a but nearly gone in spectrum b. Simultaneously, the Si−CH_2 peak emerged in spectrum b. This confirms that the hydrosilylation proceeded as expected, replacing C═C and Si−H bonds with Si−C bonds. Notably, the Si−O peak at ∼1080 cm^{-1}, a very strong absorption for silicon oxide, is quite small, even though the nanoparticles have been dried in air.

The PA-terminated Si nanoparticles were transferred into water by two methods: (1) dialysis and (2) evaporation of acrylic acid followed by redispersion of the nanoparticles in water using ultrasonication. In the latter method, long ultrasonication times (several hours) were required for dispersing the nanoparticles in water, and this appeared to lead to oxidation of the particle surfaces. Stable dispersions of the nanoparticles in water were obtained by both methods. Curves c and d in Figure 4 show the FTIR spectra of the nanoparticles transferred into deionized (DI) water by dialysis (c) and by solvent evaporation followed by ultrasonication (d). Both spectra have peaks attributed to carboxyl groups and Si−CH_2 bonds, indicating that the PA termination remains present. Spectrum d has a broad Si−O peak, indicating that part of the PA-terminated surface was incompletely oxidized after prolonged ultrasonic irradiation in water. No clear Si−O peak was observed in spectrum c, but it is possible that a small Si−O peak is hidden in the tail of the C−O peak at ∼1200 cm^{-1}.

The optical absorption, PL, and PLE spectra of the Si nanoparticles are shown in Figure 5. Spectra a−e correspond to samples 1−5, respectively, shown in Figure 2b. The weak absorbance that gradually increases with increasing energy, starting from the point marked with a black arrow, is characteristic of absorption across the indirect band gap of silicon. This absorption increases in energy with decreasing particle size but remains indirect in character. With increased

(35) Socrates, G. *Infrared and Raman Characteristic Group Frequencies: Tables and Charts*, 3rd ed.; Wiley: New York, 2001.

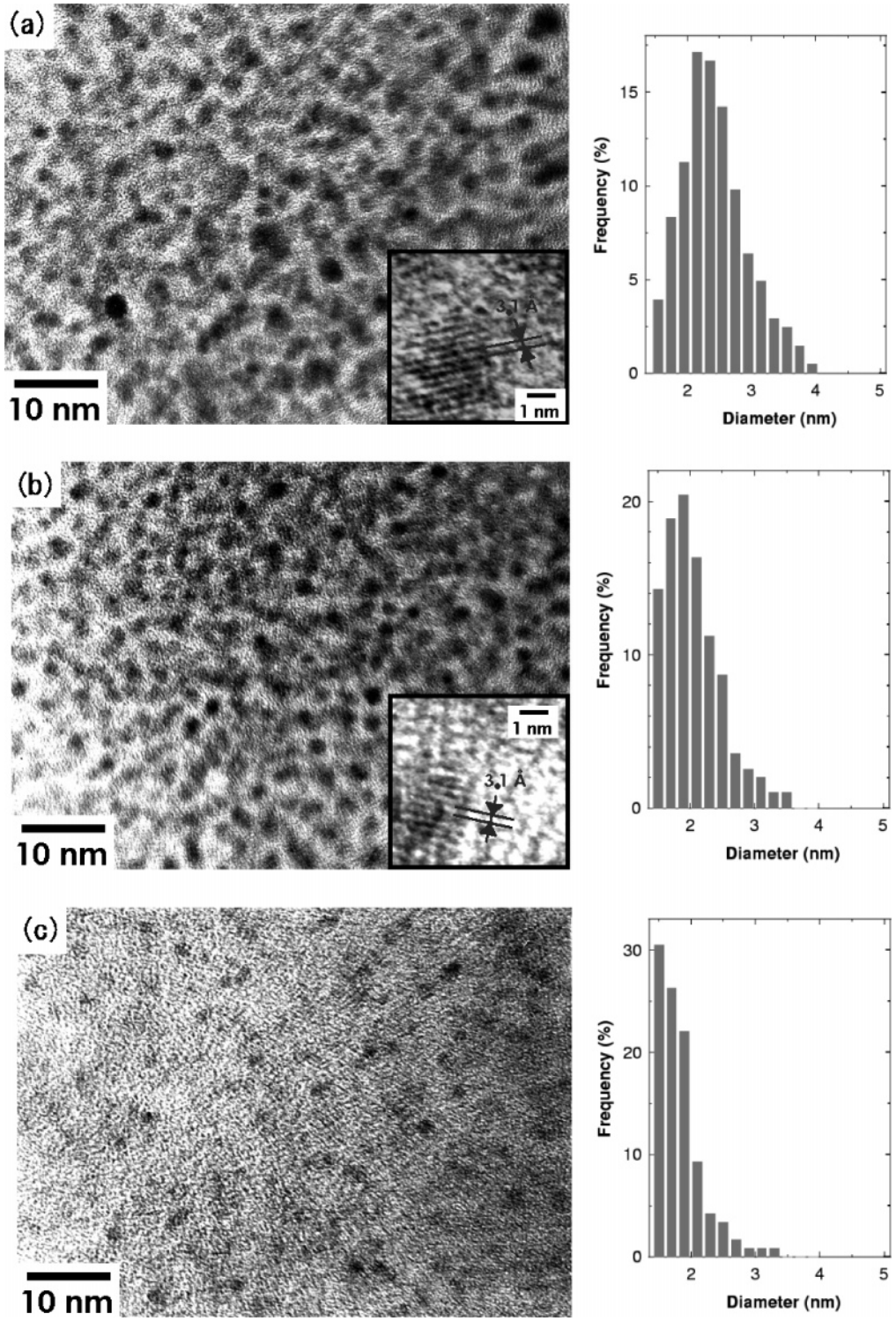

Figure 3. TEM images and size distributions obtained from TEM images, for the Si nanocrystals after hydrosilylation. Images in parts a−c correspond to samples 1−3, respectively, in Figure 2b. The insets are typical lattice images of the Si nanocrystals.

etching time (decreasing particle size), the absorption edge and the PL peak blue-shifted from 1.82 to 2.09 eV and from 2.22 to 2.52 eV, respectively. The PL shift was easily observable as a continuous change of emission color from yellow to green, as shown in the inset photograph in Figure 5 (first three samples from the left). The absorption shift of ~0.3 eV seems to be due to the increase in band-gap energy as a result of the confinement effect of the electron−hole pairs in the Si nanocrystals. Although the PL shows a similar blue shift of 0.3 eV, this does not guarantee that the intense PL is a result of band-to-band recombination, because it is located in the energy range of the indirect interband transition, and as such, may be due to the recombination via radiative centers at the nanocrystal surfaces. The origin of these radiative centers, however, is still unclear. Possible origins are surface states, defects, surface Si−C bonds, etc.[36] The similarity of the blue shift of the absorption onset and

(36) Cullis, A. G.; Canham, L. T.; Calcott, P. D. J. *J. Appl. Phys.* **1997**, *82*, 909−965.

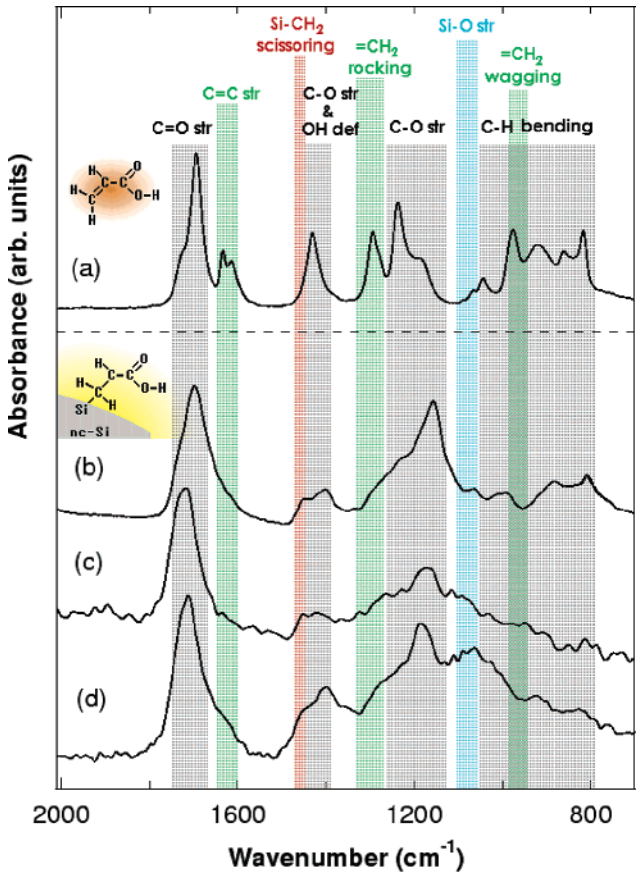

Figure 4. FTIR spectra of (a) acrylic acid and (b) the Si nanoparticles after hydrosilylation. Nanoparticles transferred to DI water after hydrosilylation by (c) dialysis and (d) evaporating the suspension and redispersing the residual nanoparticles in DI water by ultrasonic irradiation for 5 h.

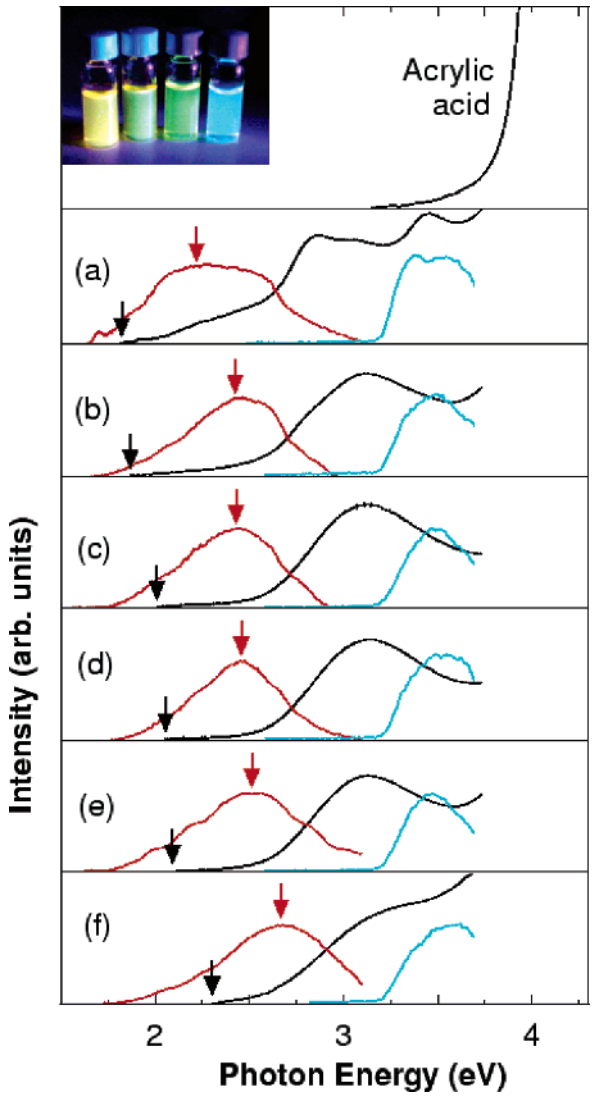

Figure 5. PL (red curves), optical absorption (black curves), and PLE (blue curves) spectra of the PA-terminated Si nanoparticles. Spectra in a−e correspond to samples 1−5, respectively, in Figure 2b. (f) PA-terminated Si nanoparticles dispersed in DI water by solvent evaporation and ultrasonication in water for 5 h. The red and black arrows indicate PL peak and absorption edge positions, respectively. The inset photograph shows (from left) PL from samples whose spectra are shown in (a), (b), (e), and (f) (excitation light: 360 nm).

PL maximum suggests that even if emission does not arise from recombination within the nanocrystal core, the energy of the states through which radiative recombination occurs is linked to the indirect band-gap energy. The PLE spectra for all samples show a sharp rise at ~3.2 eV and a peak at 3.4−3.6 eV. This corresponds to the direct interband transition at Γ ($\Gamma_{25} \rightarrow \Gamma_{15}$) in Si nanocrystals.[16] Therefore, we suggest that the intense PL results from efficient generation of electron−hole pairs in the Si nanocrystals via direct transition at Γ, followed by recombination within the nanocrystal core via an indirect transition or through surface states whose energies are coupled to the indirect band-gap energy.

As mentioned above, TEM observations indicated that the nanoparticles in samples 4 and 5 of Figure 2b, which correspond to spectra d and e, respectively, in Figure 5, were less than 1.5 nm in diameter. Nevertheless, the peak of the PL did not reach the blue region of the spectrum, even for these samples. Further increasing the etching time did not cause a further blue shift from green to blue emission, but led only to a gradual decrease in the PL emission intensity while maintaining the green emission color. Our tentative explanation for this is that radiative centers corresponding to blue PL may not exist on the surfaces of these Si nanocrystals.

Although blue PL did not result from extending the etching time, intense blue PL from the nanoparticles was observed after prolonged ultrasonication in water (spectrum f in Figure 5). This sample was prepared as follows: After evaporating the solvent from sample 5 of Figure 2b (with spectra shown in Figure 5e), we immersed the dry nanoparticles in DI water and ultrasonicated them for 5 h. After this process, the absorption edge energy shifted to 2.30 eV, and the PL peak energy increased to 2.67 eV. This blue PL is strong enough to be easily seen with the naked eye (the rightmost sample in the inset photograph in Figure 5) and is comparable in intensity to that from the yellow- and green-emitting samples. An FTIR spectrum from this blue-emitting sample was shown as curve d in Figure 4. On the basis of the increased Si−O absorption seen in that FTIR spectrum, the blue shift of the absorption edge and the PL peak seem to be attributable to surface oxidation. This is consistent with a recent report that blue-emitting silicon nanocrystals can be prepared via controlled thermal or photoinitiated surface oxidation of yellow-emitting particles that have a monolayer

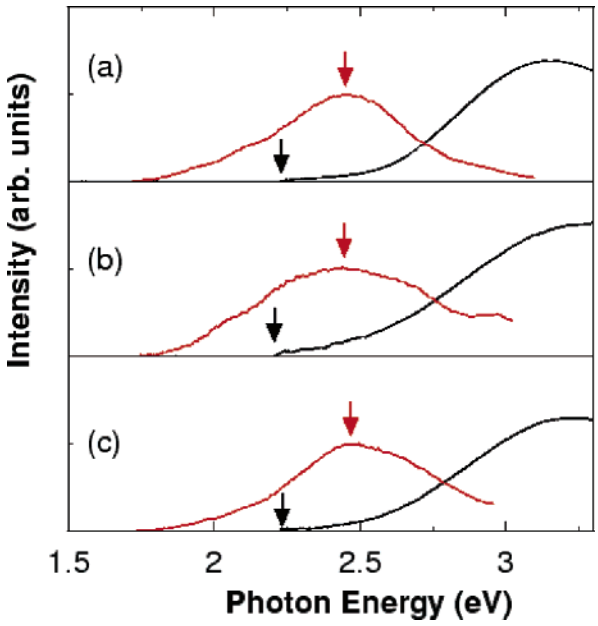

Figure 6. PL (red) and optical absorption (black) spectra of the PA-terminated Si nanoparticles (a) before and (b) after dialysis in DI water and (c) in methanol.

of organic molecules grafted to their surfaces.[37] The PLE spectrum of the blue-emitting sample after ultrasonication remains quite similar to that of the oxide-free samples. This suggests that the carrier generation mechanism remains the same, but that the recombination mechanism has changed. That is, the electron−hole pairs are still produced in the Si nanocrystals by direct transition at Γ, but then recombine at new oxygen-related surface recombination sites not present in the other samples.

Figure 6 shows the optical absorption and PL spectra of the PA-terminated Si nanoparticles transferred into DI water or methanol by dialysis. Before dialysis, the absorption edge (black arrow) and PL peak (red arrow) energies of the nanoparticles are 2.23 and 2.45 eV, respectively. When these Si nanoparticles are transferred into DI water or methanol by dialysis, the absorption edge and PL peak energies are 2.22 and 2.45 eV in either suspension. This means that the optical properties of the PA-terminated nanoparticles dispersed in DI water or methanol are essentially the same as those in acrylic acid before dialysis. These Si nanoparticles have thus far remained stably dispersed in DI water and methanol, without losing their photoluminescence, for more than two months.

(37) Hua, F.; Erogbogbo, F.; Swihart, M. T.; Ruckenstein, E. *Langmuir* **2006**, *22*, 4363−4370.

Summary

Water-dispersible propionic acid (PA)-terminated Si nanoparticles were prepared by photoinitiated hydrosilylation. The average diameter of the Si nanocrystals was 2.4 nm or less. The size and corresponding PL emission color were controlled by varying the etching time. PL emission from the PA-terminated Si nanoparticles changed continuously from yellow to green with increasing etching time. Further increasing the etching time did not produce blue-emitting nanoparticles even though the nanocrystals seemed to become less than 1.5 nm in diameter. However, strong blue emission was observed after prolonged ultrasonication of the PA-terminated Si nanoparticles in water. FTIR spectroscopy showed that surface oxidation occurred during ultrasonication. Thus, the blue luminescence seems to be attributable to radiative centers originating in the incomplete surface oxide. We suggest that all of the strong visible light emission observed in this study was a result of recombination of electron−hole pairs generated in the Si nanocrystals by the direct transition at Γ. In the blue-emitting particles, this recombination almost certainly occurs at the surface of the incompletely oxidized nanocrystals, via centers that are not present prior to oxidation. For particles emitting at longer wavelengths, recombination may occur across the indirect band gap within the nanocrystal, or via surface states whose energies are coupled to the indirect band-gap energy. By using dialysis, we dispersed the Si nanoparticles in water or methanol without changing their optical absorption and luminescence characteristics.

Acknowledgment. We thank DENKA Co. for supplying SiO_x powder and Dr. Liping Guo for help with the TEM observations. This study was supported by the Yoshida Foundation for Science and Technology, the Sasakawa Scientific Research Grant from the Japan Science Society, and The University at Buffalo Foundation Sterbutzel Research Fund.

CM060750T